Jpn J Radiol (2012) 30:296–309
DOI 10.1007/s11604-011-0047-2

ORIGINAL ARTICLE

Characteristic magnetic resonance features of focal autoimmune pancreatitis useful for differentiation from pancreatic cancer

Yukiko Sugiyama · Yasunari Fujinaga · Masumi Kadoya · Kazuhiko Ueda · Masahiro Kurozumi · Hideaki Hamano · Shigeyuki Kawa

Received: 21 July 2011 / Accepted: 19 December 2011 / Published online: 12 January 2012

Abstract
Purpose To identify characteristic magnetic resonance (MR) features of focal autoimmune pancreatitis (f-AIP) useful for differentiation from pancreatic cancer (PC).
Methods We retrospectively analyzed MR imaging findings of 20 f-AIP lesions and 40 PC lesions smaller than 40 mm in diameter. On fat-suppressed T2-weighted images and dynamic contrast-enhanced fat-suppressed T1-weighted images (DCE-T1WI), we classified MR features of internal signal intensity for each lesion into homogeneous, speckled, or target type. We assessed the sensitivity, specificity, and accuracy of these findings in the diagnosis of f-AIP. We also investigated the incidence of previously reported findings for differentiation between f-AIP and PC.
Results Speckled enhancement within a hypointense or isointense lesion on pancreatic phase DCE-T1WI (speckled type) was observed more frequently in f-AIP than in PC, with high sensitivity, high specificity, and high accuracy. Hypointensity to hyperintensity surrounding a less enhanced focal area on DCE-T1WIs (target type) and upper stream main pancreatic duct dilatation were observed more frequently in PC than in f-AIP.
Conclusion Speckled enhancement inside an f-AIP lesion on pancreatic phase DCE-T1WI was useful for differentiation from PC.

Keywords Magnetic resonance imaging · Pancreas · Pancreatitis · Autoimmune pancreatitis · Pancreatic cancer

Y. Sugiyama (✉) · Y. Fujinaga · M. Kadoya · K. Ueda · M. Kurozumi
Department of Radiology, Shinshu University School of Medicine, 3-1-1 Asahi, Matsumoto 390-8621, Japan
e-mail: ysgym@shinshu-u.ac.jp

H. Hamano
Department of Medicine, Gastroenterology, Shinshu University School of Medicine, Matsumoto, Japan

S. Kawa
Center for Health, Safety and Environmental Management, Shinshu University, Matsumoto, Japan

Introduction

Autoimmune pancreatitis (AIP) is a unique form of chronic pancreatitis in which autoimmune mechanisms are involved in the pathogenesis, with abundant lymphoplasmacytic infiltrations and fibrosis. AIP is clinically characterized by preponderance in elderly males, minimal abdominal pain, elevated serum immunoglobulin G4 (IgG4) level, and a favorable clinical response to corticosteroid therapy [1–12]. However, obstructive jaundice, body weight loss, and elevated serum level of CA19-9, or pancreatic masses generally indicative of pancreatic cancer (PC), are often observed in AIP.

Previously reported characteristic imaging findings of AIP are:

- irregular narrowing of the main pancreatic duct (MPD);
- a capsule-like rim with low density on computed tomography (CT);
- hypointensity on T2-weighted magnetic resonance (MR) images;
- diffuse enlargement of the pancreas with diminished signal intensity on T1-weighted MR images; and
- delayed parenchymal enhancement on dynamic CT or MR imaging [1–14].

These findings are, however, recognized as characteristic findings in the diffuse type of AIP. Recently, different

types of AIP, observed as a focal or segmental form of the lesion, have been reported [10–12]. It is often difficult to differentiate the focal form of AIP (f-AIP) from PC on diagnostic imaging and many patients with f-AIP have undergone unnecessary pancreatic resections on the basis of incorrect diagnosis of PC [3, 15–19]. Some authors have reported that endoscopic ultrasound (EUS)-guided fine-needle aspiration biopsy (EUS-FNAB) is an useful method for diagnosis of a focal pancreatic lesion, for example f-AIP, which is difficult to differentiate from PC [20, 21]. However, this method is invasive and inadequate specimens may lead to a misdiagnosis. MR imaging is non-invasive and has excellent tissue contrast among various diagnostic modalities. More specific diagnostic imaging is therefore required for differentiation between f-AIP and PC.

In this study, our objective was to identify MR features useful for differentiation of f-AIP from PC to avoid unnecessary pancreatectomies and EUS-FNAB for f-AIP.

Materials and methods

Subjects

This study was planned to evaluate MR findings obtained for patients with f-AIP and PC. Between August 2002 and April 2009, we retrospectively reviewed a consecutive database of abdominal MR imaging in our hospital and affiliated hospitals. Sixty-two patients had been clinically diagnosed with AIP on the basis of the revised Japanese clinical diagnostic criteria for AIP [22]. Sixty-eight patients underwent surgical resection and were histopathologically proven to have pancreatic adenocarcinoma.

Of these 130 pancreatic patients, we identified 59 patients with 60 lesions who had a focal mass smaller than 40 mm in diameter on MR images. This case selection was based on a previous report that surgical resection was not feasible, because of poor prognosis, when tumor diameter was greater than 40 mm [23]. The sample consisted of 19 f-AIP patients (13 men and 6 women; age range 47–79 years; mean age 64 years) and 40 PC patients (28 men and 12 women; age range 35–81 years; mean age 65 years). One AIP patient had two focal lesions and the other patients had one each. All 60 lesions of f-AIP and PC were measured by use of a commercial software package, EV Insite (PSP, Tokyo, Japan). The distribution of tumor size, based on the classification of pancreatic carcinoma by Japan Pancreatic Society [24], was: TS_1 (20 mm or less in the greatest dimension), one f-AIP and 15 PC; and TS_2 (20–40 mm), 19 f-AIP and 25 PC. The mean diameter of f-AIP lesions was 30.4 (19–40) mm whereas that of PC was 22.5 (10–37) mm. The mean diameter of PC was significantly smaller than that of f-AIP ($P = 0.0001$). The locations of the f-AIPs were: 16 in the head, one in the body, and three in the tail. The locations of the PCs were: 26 in the head, 13 in the body, and one in the tail.

In serological tests, 17 of 18 f-AIP patients and none of seven PC patients had increased levels of IgG4 (>105 mg/dl). Six of 17 f-AIP patients and one of six PC patients had positive rheumatoid factor ($R_F > 20$ IU/ml). Positive antinuclear antibodies (ANA > ×80) were observed in four of 16 f-AIP patients. Serum CEA (<2.5 ng/ml) was >5 ng/ml in three of 17 f-AIP patients and ten of 39 PC patients. The serum CA19-9 level (<37 U/ml) was elevated to >100 U/ml in two of 16 f-AIP patients and 18 of 39 PC patients.

MR imaging technique

MR examinations were performed with a 1.5-T system (Magnetom Symphony and Avanto; Siemens Medical Systems, Erlangen, Germany) for 13 f-AIP and 23 PC patients, and with a 3-T system (Magnetom Trio; Siemens Medical Systems) for 6 f-AIP and 17 PC patients. MR cholangiopancreatography (MRCP) was performed for 15 f-AIP and 35 PC patients.

MR images were obtained by use of a body-array coil. Software used for the study was included with the scanners as standard equipment. The sequences performed in the transverse plane were: fat-suppressed turbo spin echo sequence with respiratory-triggering for T2-weighted images (T2WI) and fat-suppressed 2D-gradient echo (GRE) fast low-angle shot (FLASH) sequence with breath-holding or fat-suppressed 3D-GRE volume interpolated breath-hold examination (VIBE) for T1-weighted images (T1WI). 2D-GRE FLASH T1WIs (2D-T1WIs) were performed for 11 f-AIP and 18 PC patients, and 3D-GRE VIBE T1WIs (3D-T1WIs) for eight f-AIP and 22 PC patients.

The settings for T2WI were: repetition time (TR)/echo time (TE) = 2030–8411.09 ms/69–91 ms; average number of signals = 2; matrix = 512 × 358–512; slice thickness = 4–8 mm; and field of view = 32–42 cm × 22.5–36 cm. The settings for 2D-T1WI were: TR/TE/flip angle (FA) = 132–193 ms/2.05–2.64 ms/70°–90°; average number of signals = 1; matrix = 434–512 × 332–460; slice thickness = 5.0–8.0 mm; and field of view = 34–43 cm × 26.3–37.7 cm. The settings for 3D-T1WI were: TR/TE/FA = 3.39–4.85 ms/1.23–2.18 ms/13°–18°; average number of signals = 1; matrix = 512–640 × 320–448; slice thickness = 2.0–2.5 mm; and field of view = 38–44 cm × 25.9–35.0 cm. MRCP images were acquired with the rapid acquisition and relaxation enhancement (RARE) method (TR/TE = 850–6625.91 ms/451–980 ms, matrix = 512 × 512). Pre-contrast and dynamic contrast-enhanced T1WIs (DCE-T1WI) were available for all patients, but fat-suppressed T2WIs were not available for one AIP patient.

DCE-T1WIs were obtained sequentially after intravenous bolus administration of meglumine gadopentetate (Magnevist, Bayer Schering Pharma, Berlin, Germany) or gadodiamide hydrate (Omniscan, Daiichi-Sankyo Pharma, Tokyo, Japan) at 0.2 ml/kg body weight and a rate of 3 ml/s by use of a power injector, followed by flushing with 40 ml physiological saline solution at the same rate. After the start of the bolus injection, a pancreatic phase image was acquired at 40 s, and an equilibrium phase image at 100 s.

Imaging analysis

First, we characterized the internal signal intensity of the pancreatic lesions relative to the surrounding pancreatic parenchyma, and classified the MR findings into three types—homogeneous type, speckled type, and target type (Fig. 1). Homogeneous type lesions were homogeneously hypointense to hyperintense areas on T2WI or precontrast T1WI, or homogeneous enhanced areas on DCE-T1WI (Fig. 1a, b). Speckled type lesions were hypointense or isointense areas including speckled or dotted hyperintense areas on T2WI or precontrast T1WI, or hypointense or isointense areas including speckled or dotted enhanced areas on DCE-T1WI (Fig. 1c). Target type lesions were hyperintense surrounding a more hyperintense focal area on T2WI (Fig. 1d), or hypointense to hyperintense surrounding a more hypointense area either on precontrast T1WI or hypointense to hyperintense surrounding a more less enhanced area on DCE-T1WI (Fig. 1e). Target type was distinguished from capsule-like rim [13] that possibly corresponded to an inflammatory process involving peripancreatic tissues. The differences in the incidence of these three types between f-AIP and PC were assessed, and sensitivity, specificity, and accuracy were calculated for the usefulness of each type of MR feature in the diagnosis of f-AIP.

Second, we assessed previously reported findings for differentiation between f-AIP and PC, for example marginal unambiguity of the lesion, the incidence of vascular involvement, capsule-like rim [13], duct penetrating sign [25], and dilatation of the upper stream MPD [26, 27]. The incidence of the duct penetrating sign and MPD dilatation was evaluated only on MRCP. The other findings were assessed by reviewing all images of all sequences. Vascular involvement was defined as positive when the lesion was in contact with a celiac artery, common hepatic artery, superior mesenteric artery, and/or splenic artery, and when the portal vein, superior mesenteric vein, or splenic vein narrowed in the pancreatic lesions on any MR image. Although there are no strict criteria for diagnosis of MPD dilatation, if the MPD measures greater than 3 mm in the head and 2 mm in the body or tail of the pancreas, it is usually regarded as enlarged at Emory University Hospital [28]. The differentiation of the above findings between f-AIP and PC was evaluated qualitatively.

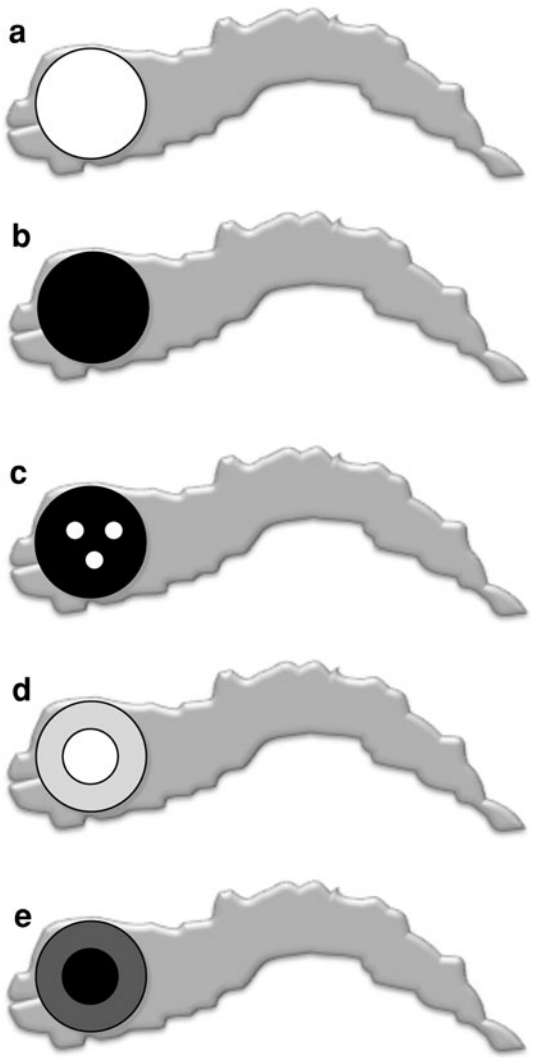

Fig. 1 Schematic illustrations of each type of focal pancreatic lesion. **a** The homogeneous type MR feature. The lesion is homogeneously hyperintense compared with normal pancreatic parenchyma. **b** The homogeneous type MR feature. The lesion is homogeneously hypointense. **c** The speckled type MR feature. The lesion is hypointense and includes speckled or dotted hyperintense areas or enhancement. **d** The target type MR feature. The lesion has a hyperintense region surrounding a more hyperintense focal area and looks like a target. **e** The target type MR feature. The lesion has a hypointense region surrounding a more hypointense or less enhanced focal area

All of the images for each patient were shown in random order with the observers unaware of the diagnosis; they were evaluated by consensus of three radiologists with 5, 18, and 33 years of abdominal imaging experience. When the readers evaluated one sequence, they were allowed to refer to images of other sequences and CT images because

the purpose of this study was analysis of imaging features, not lesion detectability.

Statistical analysis

Fisher's exact test was used to assess any differences. A value of $P < 0.05$ was considered significant. All statistical analysis was performed with a statistical software package (Prism, version 4; GraphPad Software, CA, USA).

Results

The distributions of pancreatic lesions with regard to types of MR feature are shown in Table 1. In the comparison of f-AIP with PC, the homogeneous type lesions on equilibrium phase DCE-T1WI, and the speckled type lesions on T2WI, precontrast T1WI, pancreatic phase DCE-T1WI, and equilibrium phase DCE-T1WI were observed significantly more frequently in f-AIP than in PC ($P < 0.05$). In contrast, the homogeneous type on T2WI and precontrast T1WI, and the target type lesions DCE-T1WI were observed significantly more frequently in PC than in f-AIP ($P < 0.05$). The target type MR feature was not observed on any sequence for patients with f-AIP.

The sensitivity, specificity, and accuracy of each type of MR feature for diagnosing f-AIP and PC are shown in Table 2. Regarding diagnosis of f-AIP, the MR features with high sensitivity were the speckled type on pancreatic phase DCE-T1WI (85.0%) and equilibrium phase DCE-T1WI (75.0%). The MR features with high specificity were the speckled type on T2WI (97.5%), on precontrast T1WI (97.5%), on pancreatic phase DCE-T1WI (95.0%), and on equilibrium phase DCE-T1WI (95.0%), and the target type on T2WI (82.5%) and on precontrast T1WI (82.5%). The MR features with high accuracy were the speckled type on T2WI (83.1%), on precontrast T1WI (83.3%), and on pancreatic phase DCE-T1WI (91.7%). Regarding diagnosis of PC, the MR features with high sensitivity were the homogeneous type on T2WI (80.0%) and on precontrast T1WI (80.0%). The MR features with high specificity were the homogeneous type on pancreatic phase DCE-T1WI (85.0%), the speckled type on equilibrium phase DCE-T1WI (75.0%), and the target type on all sequences (100%). The MR feature with high accuracy was the target type on pancreatic phase DCE-T1WI (75.0%).

In the comparison between 2D-T1WI and 3D-T1WI, homogeneous type lesions on pancreatic phase 3D DCE-T1WI were observed significantly more frequently than on 2D-T1WI for PC patients ($P = 0.0455$). There was no

Table 1 Distributions of pancreatic lesions with regard to types of MR feature

Types of MR feature	No. of lesions (%)	
	Autoimmune pancreatitis ($n = 20$)	Pancreatic cancer ($n = 40$)
T2WI[a]		
Homogeneous type[b]	9 (47.3)	32[†] (80.0)
Speckled type[c]	10[‡] (52.6)	1 (2.5)
Target type[d]	0 (0)	7 (17.5)
Precontrast T1WI		
Homogeneous type	9 (45.0)	32[†] (80.0)
Speckled type	11[‡] (55.0)	1 (2.5)
Target type	0 (0)	7 (17.5)
Pancreatic phase contrast-enhanced T1WI		
Homogeneous type	3 (15.0)	13 (32.5)
Speckled type	17[‡] (85.0)	2 (5.0)
Target type	0 (0)	25[‡] (62.5)
Equilibrium phase contrast-enhanced T1WI		
Homogeneous type	15[†] (75.0)	14 (35.0)
Speckled type	5[†] (25.0)	2 (5.0)
Target type	0 (0)	24[‡] (60.0)

[†] $P < 0.05$, [‡] $P < 0.001$; the number of lesions is significantly larger than for the other disease

[a] T2WI was not available for one autoimmune pancreatitis patient

[b] Homogeneous type: a homogeneous hypointense to hyperintense lesion on any sequence

[c] Speckled type: a hypointense or isointense lesion including speckled or dotted hyperintense areas

[d] Target type: a hyperintense lesion surrounding a more hyperintense focal area on fat-suppressed T2WI or a hypointense to hyperintense lesion surrounding a more hypointense area on precontrast or on contrast-enhanced T1WI

Table 2 Sensitivity, specificity, and accuracy of each type of MR feature in the diagnosis of autoimmune pancreatitis and pancreatic cancer

Types of MR feature	Autoimmune pancreatitis			Pancreatic cancer		
	Sens. (%)	Spec. (%)	Accu. (%)	Sens. (%)	Spec. (%)	Accu. (%)
T2WI[a]						
Homogeneous type[b]	47.4	20.0	28.8	80.0	52.6	71.2
Speckled type[c]	52.6	97.5	83.1	2.5	47.4	16.9
Target type[d]	0.0	82.5	55.9	17.5	100.0	44.1
Precontrast T1WI						
Homogeneous type	45.0	20.0	28.3	80.0	55.0	71.7
Speckled type	55.0	97.5	83.3	2.5	45.0	16.7
Target type	0.0	82.5	55.0	17.5	100.0	45.0
Pancreatic phase contrast-enhanced T1WI						
Homogeneous type	15.0	67.5	50.0	32.5	85.0	50.0
Speckled type	85.0	95.0	91.7	5.0	15.0	8.3
Target type	0.0	37.5	25.0	62.5	100.0	75.0
Equilibrium phase contrast-enhanced T1WI						
Homogeneous type	75.0	65.0	68.3	35.0	25.0	31.7
Speckled type	25.0	95.0	71.7	5.0	75.0	28.3
Target type	0.0	40.0	26.7	60.0	100.0	73.3

Sens. sensitivity, *Spec.* specificity, *Accu.* accuracy

[a] T2WI was not available for one autoimmune pancreatitis patient

[b] Homogeneous type: a homogeneous hypointense to hyperintense lesion on all sequences

[c] Speckled type: a hypointense or isointense lesion including speckled or dotted hyperintense areas

[d] Target type: a hyperintense lesion surrounding a more hyperintense focal area on fat-suppressed T2WI or a hypointense to hyperintense lesion surrounding a more hypointense area on precontrast or on contrast-enhanced T1WI

other finding for which the incidence was significantly different between 2D-T1WI and 3D-T1WI (Table 3).

The sensitivity, specificity, and accuracy of each type of MR feature for diagnosis of f-AIP and PC compared with 2D-T1WI and 3D-T1WI are shown in Table 4. In diagnosis of f-AIP, both on 2D and 3D sequences, the speckled type MR features on pancreatic phase DCE-T1WI were highly sensitive (2D 81.8%, 3D 88.9%), the speckled type MR features on precontrast T1WI, on pancreatic phase DCE-T1WI, and on equilibrium phase DCE-T1WI were highly specific (2D 94.7%, 3D 100%; 2D 89.5%, 3D 100%; 2D 89.5, 3D 100%), and the speckled type MR features on pancreatic phase DCE-T1WI were highly accurate (2D 86.7%, 3D 96.7%). In diagnosis of PC, both on 2D and 3D sequences, the homogeneous type MR features on pancreatic phase DCE-T1WI were highly specific (2D 81.8%, 3D 88.9%) and the target type MR features on precontrast T1WI, on pancreatic phase DCE-T1WI, and on equilibrium phase DCE-T1WI were highly specific (2D 100%, 3D 100%; 2D 100%, 3D 100%; 2D 100%, 3D 100%).

Regarding the homogeneous type, nine f-AIP lesions appeared as this type on T2WI, four of which were the same type on precontrast T1WI. Nine f-AIP lesions appeared as the homogeneous type on precontrast T1WI; two of these were the same type on pancreatic phase DCE-T1WI and seven were the same type on equilibrium phase DCE-T1WI (Fig. 2). Thirty-two PC lesions appeared as the homogeneous type on T2WI; 28 of these were the same type on precontrast T1WI. Thirty-two PC lesions appeared as the homogeneous type on precontrast T1WI; 13 of these were the same type on pancreatic phase DCE-T1WI and 11 were the same type on equilibrium phase DCE-T1WI.

Regarding the speckled type, ten f-AIP lesions appeared as this type on T2WI, and six of these were the same type on precontrast T1WI. Eleven f-AIP lesions appeared as the speckled type on precontrast T1WI; 10 of these were the same type on pancreatic phase DCE-T1WI and four were the same type on equilibrium phase DCE-T1WI (Fig. 3). In addition, we found three f-AIP lesions with speckled hyperintense areas on precontrast T1WI corresponding to those on pancreatic phase DCE-T1WI (Fig. 4). One PC lesion that appeared as the speckled type on T2WI was not the same type on precontrast T1WI. One PC lesion appeared as the speckled type on precontrast T1WI, although it had appeared as the target type, not the same speckled type, on DCE-T1WI (Fig. 5).

Table 3 Distributions of pancreatic lesions with regard to types of MR feature: comparison of 2D-T1WI and 3D-T1WI

Types of MR feature	No. of lesions (%)			
	Autoimmune pancreatitis		Pancreatic cancer	
	2D ($n = 11$)	3D ($n = 9$)	2D ($n = 19$)	3D ($n = 21$)
Precontrast T1WI				
Homogeneous type[a]	5 (45.5)	4 (44.4)	13 (68.4)	19* (90.5)
Speckled type[b]	6** (54.5)	5** (55.6)	1 (5.3)	0 (0)
Target type[c]	0 (0)	0 (0)	5** (26.3)	2 (9.5)
Pancreatic phase contrast-enhanced T1WI				
Homogeneous type	2 (18.2)	1 (11.1)	3 (15.8)	10[†] (47.6)
Speckled type	9** (81.8)	8** (88.9)	2 (10.5)	0 (0)
Target type	0 (0)	0 (0)	14** (73.7)	11* (52.4)
Equilibrium phase contrast-enhanced T1WI				
Homogeneous type	9** (81.8)	6 (66.7)	4 (21.1)	10 (47.6)
Speckled type	2 (18.2)	3* (33.3)	2 (10.5)	0 (0)
Target type	0 (0)	0 (0)	13** (68.4)	11* (52.4)

2D two-dimensional fast low angle shot T1WI, *3D* three-dimensional volume interpolated breath-hold examination T1WI

* $P < 0.05$, ** $P < 0.001$; the number of lesions is significantly larger than for the other disease

† The number of lesions on the 3D sequence is significantly larger than that on the 2D sequence ($P = 0.0455$)

[a] Homogeneous type: a homogeneous hypointense to hyperintense lesion on all sequences

[b] Speckled type: a hypointense or isointense lesion including speckled or dotted hyperintense areas

[c] Target type: a hyperintense lesion surrounding a more hyperintense focal area on fat-suppressed T2WI or a hypointense to hyperintense lesion surrounding a more hypointense area on precontrast or on contrast-enhanced T1WI

Table 4 Sensitivity, specificity, and accuracy of each type of MR feature in the diagnosis of autoimmune pancreatitis and pancreatic cancer: comparison of 2D-T1WI and 3D-T1WI

Types of MR feature	Autoimmune pancreatitis						Pancreatic cancer					
	Sens. (%)		Spec. (%)		Accu. (%)		Sens. (%)		Spec. (%)		Accu. (%)	
	2D	3D	2D	3D	2D	3D	2D	3D	2D	3D	2D	3D
Precontrast T1WI												
Homogeneous type[a]	45.5	44.4	31.6	9.5	36.7	20.0	68.4	90.5	54.5	55.6	63.3	80.0
Speckled type[b]	54.5	55.6	94.7	100	80.0	86. 7	5.3	0.0	45.5	44.4	20.0	13.3
Target type[c]	0.0	0.0	73.7	90.5	46.7	63.3	26.3	9.5	100	100	53.3	36.7
Pancreatic phase contrast-enhanced T1WI												
Homogeneous type	18.2	11.1	84.2	52.4	60.0	40.0	15.8	47.6	81.8	88.9	40.0	60.0
Speckled type	81.8	88.9	89.5	100	86.7	96.7	10.5	0.0	18.2	11.1	20.0	3.3
Target type	0.0	0.0	26.3	47.6	16.7	33.3	73.7	52.4	100	100	83.3	66.7
Equilibrium phase contrast-enhanced T1WI												
Homogeneous type	81.8	66.7	78.9	52.4	80.0	56.7	21.1	47.6	18.2	33.3	20.0	43.3
Speckled type	18.2	33.3	89.5	100	63.3	80.0	10.5	0.0	81.8	66.7	36.7	20.0
Target type	0.0	0.0	31.6	47.6	20.0	33.3	68.4	52.4	100	100	80.0	66.7

Sens. sensitivity, *Spec.* specificity, *Accu.* accuracy, *2D* two-dimensional fast low angle shot T1WI, *3D* three-dimensional volume interpolated breath-hold examination T1WI

[a] Homogeneous type: a homogeneous hypointense to hyperintense lesion on any sequence

[b] Speckled type: a hypointense or isointense lesion including speckled or dotted hyperintense areas

[c] Target type: a hyperintense lesion surrounding a more hyperintense focal area on fat-suppressed T2WI or a hypointense to hyperintense lesion surrounding a more hypointense area on precontrast or on contrast-enhanced T1WI

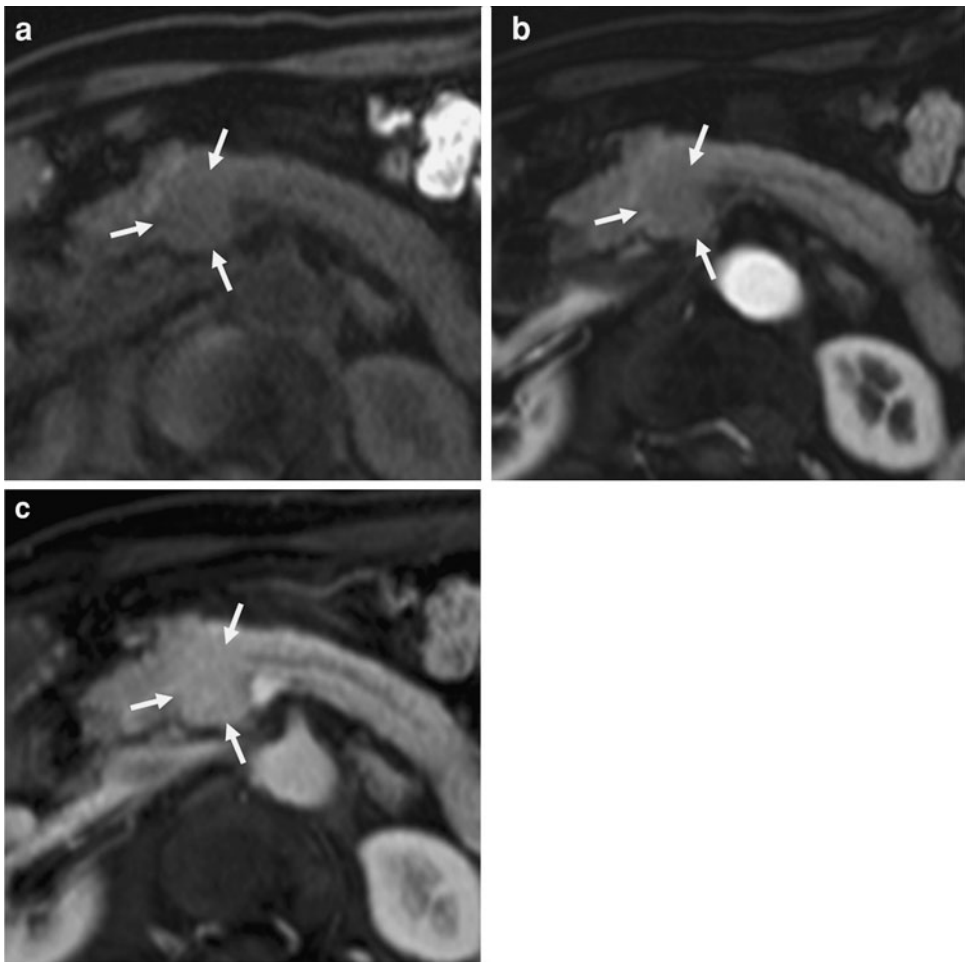

Fig. 2 A 69-year-old man had focal autoimmune pancreatitis in the head of the pancreas. **a** On the axial precontrast fat-suppressed T1-weighted MR image, a mass in the head of the pancreas is revealed as a homogeneously hypointense area (*white arrows*). This lesion is categorized as the homogeneous type. **b** On the axial pancreatic phase dynamic contrast-enhanced fat-suppressed T1-weighted MR image, a mass in the head of the pancreas is revealed as a homogeneously hypointense area (*white arrows*). This lesion is categorized as the homogeneous type. **c** On the axial equilibrium phase dynamic contrast-enhanced fat-suppressed T1-weighted MR image, a mass in the head of the pancreas is revealed as a homogeneously hypointense area (*white arrows*). This lesion is categorized as the homogeneous type

Seven PC lesions appeared as the target type on T2WI; three of these had the same appearance on precontrast T1WI, five had the same appearance on pancreatic phase DCE-T1WI, and six had the same appearance on equilibrium phase DCE-T1WI. Seven PC lesions appeared as the target type on precontrast T1WI; all of these had the same appearance on pancreatic phase DCE-T1WI and five had the same appearance on equilibrium phase DCE-T1WI (Fig. 6).

The distributions of MR findings previously reported, for example marginal unambiguity of the lesion, incidence of vascular invasion, capsule-like rim, duct penetrating sign, and dilatation of the upper stream MPD, are shown in Table 5. A significant difference between f-AIP and PC was noted for the finding MPD dilatation only ($P < 0.001$). There was no statistically significant difference in the incidence of the other findings between f-AIP and PC. Most of the f- AIP and PC lesions had an unclear margin. A capsule-like rim was recognized only in two f-AIP patients and duct-penetrating sign only in two f-AIP patients and three PC patients.

Discussion

It is very important to distinguish f-AIP from PC, because the treatments are different. Steroid therapy is effective for AIP, morphologic changes are reversible, and pancreatic function can return to normal. In contrast, operation is the standard treatment for PC. In a retrospective study of Whipple resections performed for presumed malignancy of a mass in the head of the pancreas, approximately 10% (47 of 442) were non-neoplastic benign lesions on pathological evaluation, and nearly a quarter (11 of 47) of these proved to be AIP [19]. One of the reasons unnecessary surgery was performed is the paucity of findings helpful in differentiation between f-AIP and PC, despite the fact that this unique type has also been found in 24–45% of such cases [4, 10, 16, 17, 26].

It is often difficult to distinguish f-AIP from PC, because their clinical and radiologic features often resemble each other. Elevated serum IgG4 levels are characteristic of AIP [7] and the 2006 Japanese clinical diagnostic criteria for AIP [22] include elevation of the serum IgG4 level as a

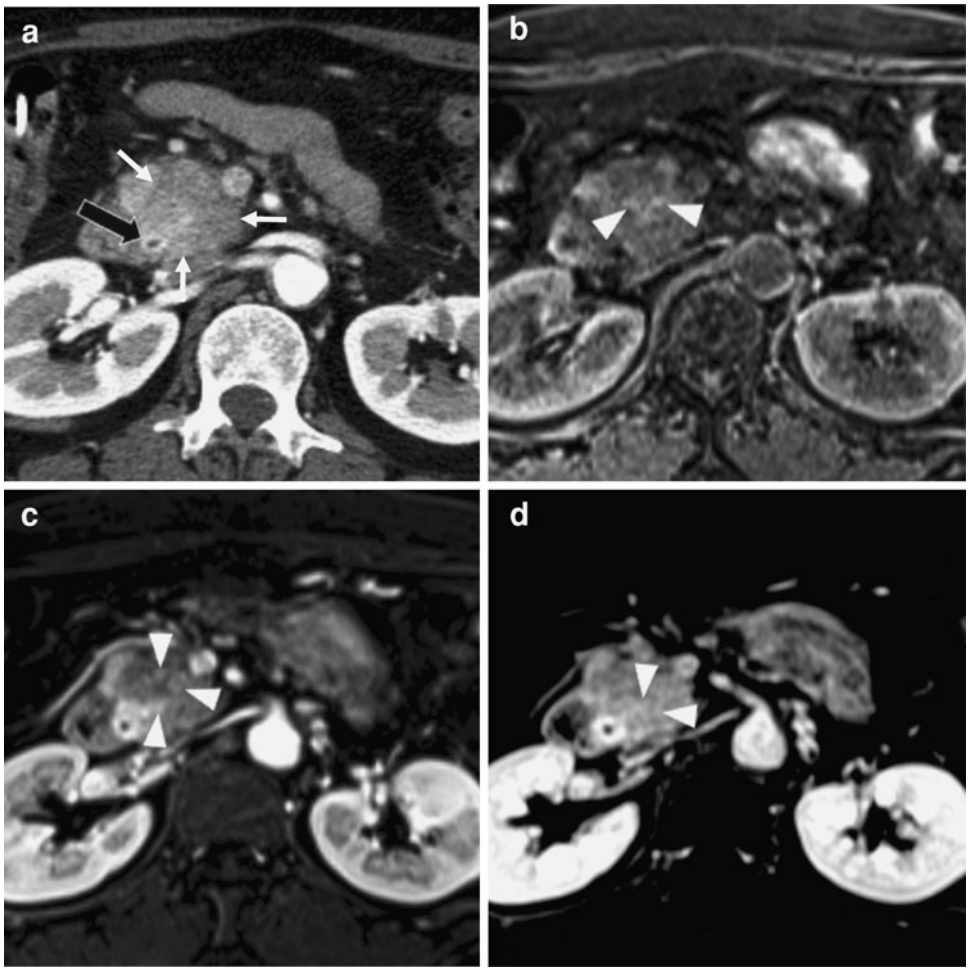

Fig. 3 A 53-year-old woman had focal autoimmune pancreatitis in the head of the pancreas. **a** Contrast-enhanced computed tomography shows a pancreatic mass lesion depicted as an inhomogeneous hypodense area (*white arrows*) and a narrowing common bile duct with wall thickening (*black arrow*). **b** On the axial precontrast fat-suppressed T1-weighted MR image, a mass in the head of the pancreas is observed as a hypointense area including speckled or dotty hyperintensity (*white arrowheads*). This lesion is categorized as the speckled type. **c** On the axial pancreatic phase dynamic contrast-enhanced fat-suppressed T1-weighted MR image, a mass in the head of the pancreas is observed as a hypointense area including speckled or dotty hyperintensity (*white arrowheads*). This lesion is categorized as the speckled type. **d** On the axial equilibrium phase dynamic contrast-enhanced fat-suppressed T1-weighted MR image, a mass in the head of the pancreas is observed as a hypointense area including speckled hyperintensity (*white arrowheads*). This lesion is categorized as the speckled type

diagnostic factor. In our study, serum IgG4 levels were elevated in 17/18 f-AIP patients, whereas they were elevated in no PC patients, and sensitivity and specificity for diagnosis of f-AIP were high. However, elevation of serum IgG4 may be also seen in PC [29, 30] and some other pathological conditions, for example atopic dermatitis [31], parasitic disease [32], pemphigus vulgaris, and foliaceus [33]. Thus, IgG4 is not always a specific marker for serological diagnosis of AIP and cannot be used alone to distinguish AIP from PC. Hardacre et al. [16] reported no statistically significant differences in the incidence of abdominal pain, weight loss, jaundice, or preoperative carcinoembryonic agent or CA 19-9 levels between f-AIP and PC. Radiologically, it has been reported that obstruction of the bile duct, vascular involvement, or delayed enhancement is frequently seen in both f-AIP and PC [17, 26, 34]. However, Kim et al. [35] maintained that the most discriminating MR feature of chronic pancreatitis was an ill-defined demarcation with relatively increased signal and enhancement, and Kawamoto et al. [27] reported that major pancreatic vascular involvement is uncommon in AIP as compared with PC in evaluation with multidetector CT. In our MR imaging study, unclear margin and vascular involvement were common in both f-AIP and PC. The differences in the frequency of these findings between the two entities were not significant ($P > 0.05$). This indicates that a low-grade inflammatory reaction in the peripancreatic region can occur in both. Thus, when an unclear margin and vascular involvement are observed in focal pancreatic enlargement, diagnosis of f-AIP should not be

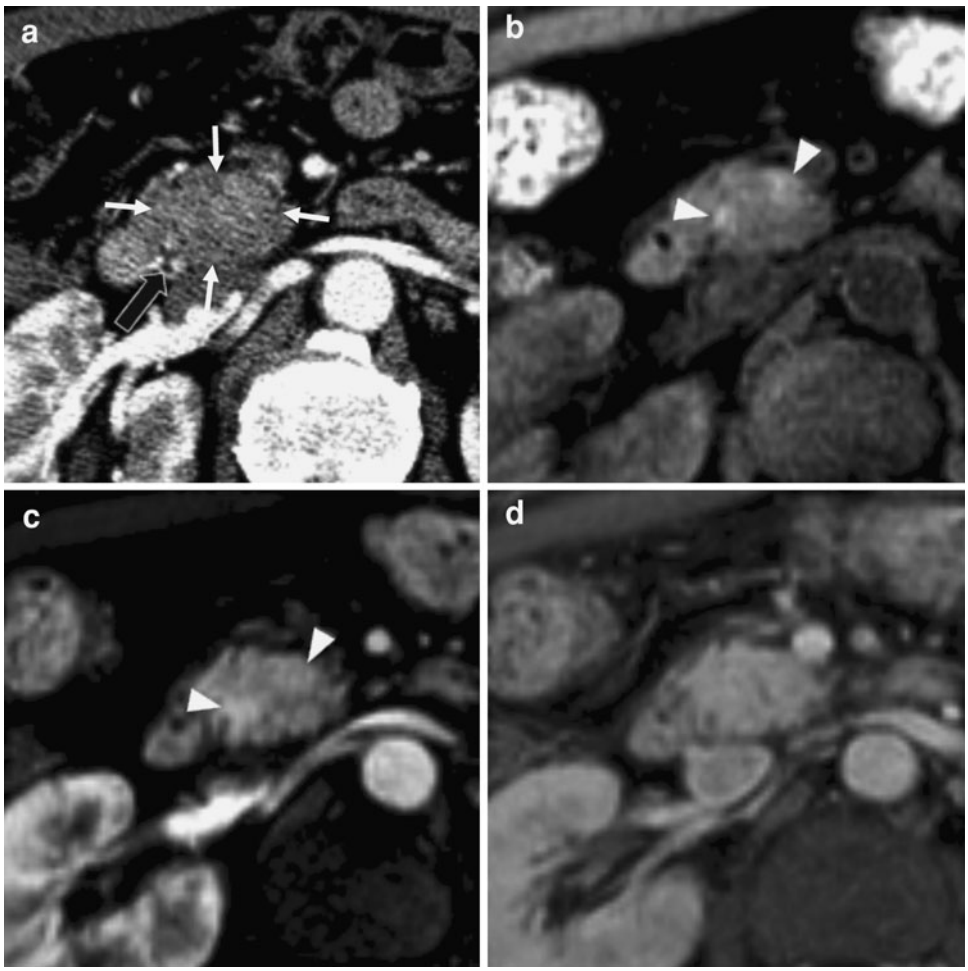

Fig. 4 A 67-year-old man had focal autoimmune pancreatitis in the head of the pancreas. **a** Contrast-enhanced computed tomography shows a pancreatic mass lesion (*white arrows*) and narrowing of common bile duct with wall thickening (*black arrow*). **b** On the axial precontrast fat-suppressed T1-weighted MR image, speckled hyperintense areas (*white arrowheads*) are recognized within the pancreas head mass (the speckled type). **c** On the axial pancreatic phase dynamic contrast-enhanced fat-suppressed T1-weighted MR image, speckled enhanced areas (*white arrowheads*) are recognized within the pancreas head mass (the speckled type). The speckled enhanced areas correspond to the speckled hyperintense areas on the precontrast fat-suppressed T1-weighted MR image shown as **b**. **d** On the axial equilibrium phase dynamic contrast-enhanced fat-suppressed T1-weighted MR image, a mass in the head of the pancreas is observed as a homogeneous isointense area (the homogeneous type)

excluded offhand without, of course, also dismissing diagnosis of PC.

The MR features previously reported as being characteristic of AIP include a capsule-like rim, duct-penetrating sign, and diffuse enlargement of the pancreas with reduced signal intensity on T1WI, increased signal intensity on T2WI, or enhancement on equilibrium phase DCE-T1WI. A capsule-like rim has been reported to be characteristic of AIP and present in 16–80% of such patients [10, 11, 13, 27]. Duct-penetrating sign on MRCP has been reported to be helpful in distinguishing an inflammatory pancreatic mass from conventional pancreatic carcinoma [25], although Kim et al. [35] indicated that this finding had low specificity (50%) for differentiation of PC from chronic pancreatitis. In our study, capsule-like rim and duct-penetrating sign were seen only in a few patients with f-AIP. Therefore, these findings may not be useful in differentiating f-AIP from PC because of low sensitivity, although they may be specific.

In our assessment of the internal signal intensity of the lesion, MR features were classified into three types: homogeneous, speckled, and target. These three types of MR finding occurred with different frequency after use of different pulse sequences.

Homogeneous delayed enhancement of the lesions of AIP has been reported in other earlier CT and MR imaging studies, and this finding reflects fibrosis or diffuse lymphocytic infiltration, which are pathological characteristics of AIP [10, 34]. Homogeneous enhancement may also be observed for sclerotic type PC, because of similar pathologic features. However, PC frequently includes necrosis or bleeding that is observed as a less or heterogeneous enhanced area even on delayed images [34]. In our study, the homogenous type MR feature on equilibrium phase 2D DCE-T1WI was observed significantly more frequently in f-AIP than in PC (Table 1), a result which may be in agreement with previous reports [10, 34]. On the other hand, there was no significant difference in incidence between the two diseases on 3D DCE-T1WI in our study. A difference of sequence may have affected visualization, although this was not a quantitative study.

In our study, we found that f-AIP could be discriminated from PC on the basis of the MR feature of speckled type on pancreatic phase DCE-T1WI. This finding was significantly

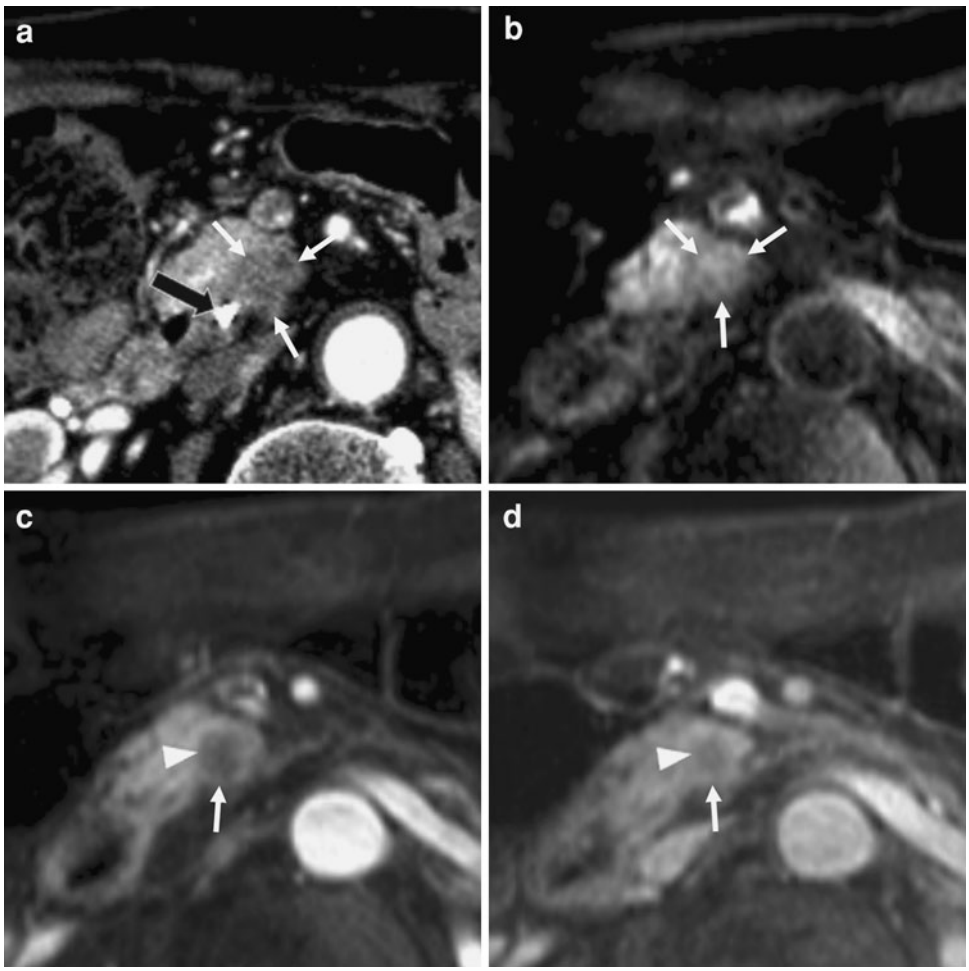

Fig. 5 A 75-year-old man had pancreatic cancer in the head of the pancreas. **a** Contrast-enhanced computed tomography shows the pancreatic cancer as a hypodense area (*white arrows*). An endoscopic nasobiliary drainage tube (*black arrow*) has been inserted into the common bile duct. **b** On the axial precontrast fat-suppressed T1-weighted MR image, a mass in the head of the pancreas (*white arrows*) is observed as a hypointense area including speckled hyperintensity. This lesion is categorized as the speckled type. **c** On the axial pancreatic phase dynamic contrast-enhanced fat-suppressed T1-weighted MR image, a mass in the head of the pancreas is apparent as a slightly hypointense area (*white arrow*) with a central poorly enhanced area (*white arrowhead*). This lesion is categorized as the target type. **d** On the axial equilibrium phase dynamic contrast-enhanced fat-suppressed T1-weighted MR image, a mass in the head of the pancreas is apparent as a slightly hyperintense area (*white arrow*) with a central poorly enhanced area (*white arrowhead*). This lesion is categorized as the target type

more frequent in f-AIP than in PC, and provided high accuracy both on 2D-T1WI and on 3D-T1WI, i.e. the reproducibility of this finding was certain to be validated. Our paper is the first to report speckled or dotted enhancement within a pancreatic lesion on pancreatic phase DCE-T1WI as a novel finding useful in discriminating f-AIP from PC. Interestingly, we found three f-AIP lesions that had speckled hyperintense areas both on precontrast T1WI and on pancreatic phase DCE-T1WI, consistent with each other (Fig. 4). We consider that speckled or dotted hyperintensity inside a pancreatic lesion on precontrast T1WI and speckled or dotted enhancement on pancreatic phase DCE-T1WI may have reflected residual normal pancreatic lobules within the f-AIP lesions. Mild involvement of inflammatory change may have also been reflected by speckled enhancement on pancreatic phase DCE-T1WI, whereas inflammatory change could have been represented as hypointensity on precontrast T1WI, because the sensitivity of the speckled type for diagnosis of f-AIP was higher on pancreatic phase DCE-T1WI than on precontrast T1WI. Fujinaga et al. [36] reported one f-AIP lesion that had speckled hyperintensity on precontrast and arterial-dominant phase contrast-enhanced T1WI, and that hyperintense areas inside a pancreatic lesion corresponded, pathologically, to residual pancreatic lobules. Chandan et al. [37] documented a high frequency of patchy involvement in pancreas with AIP, with the individual spared foci being quite large, up to 8.8 cm^2 in some cases. These reports suggest that spared pancreatic foci can be visualized as speckled or patchy hyperintensity inside an f-AIP lesion on

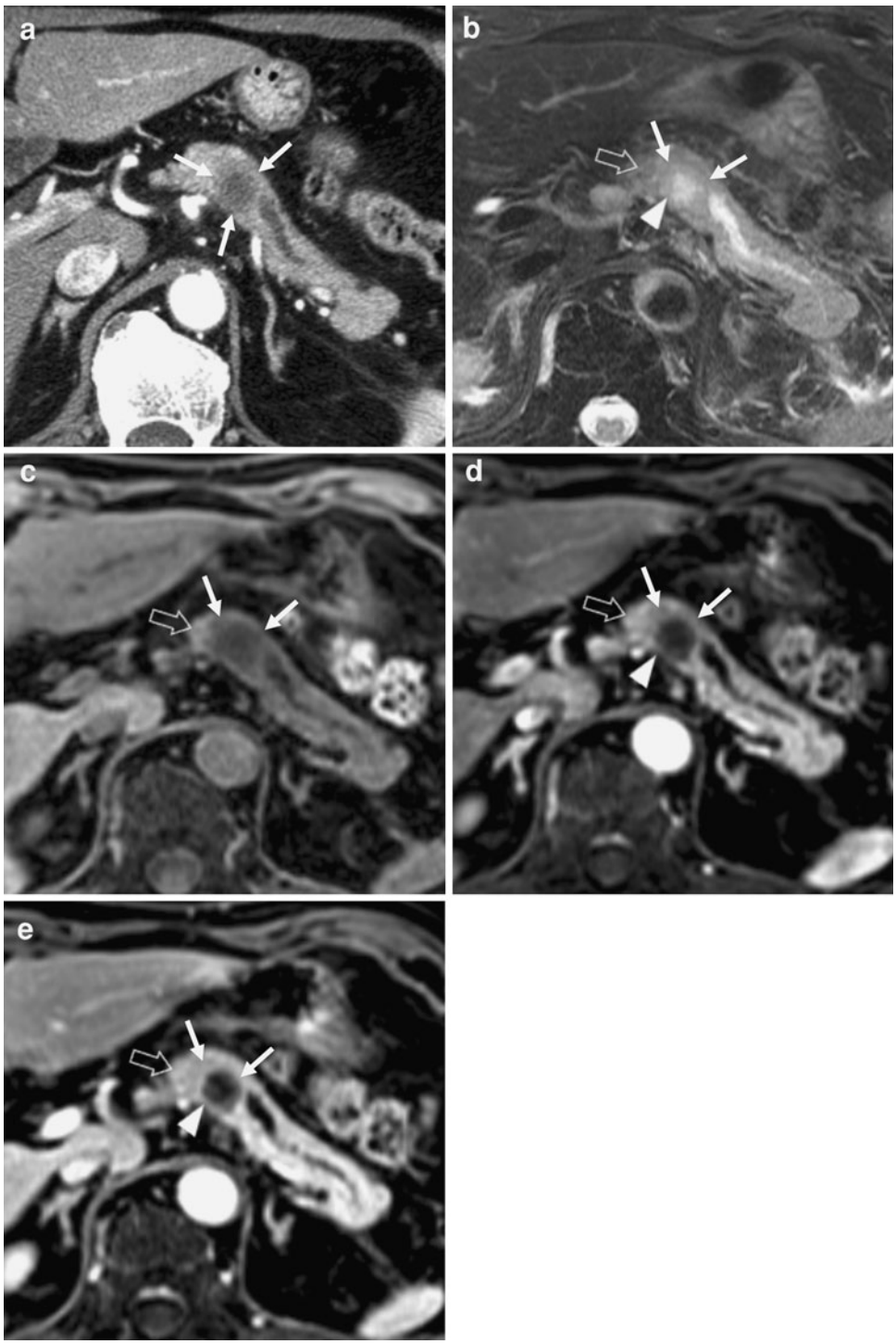

Fig. 6 A 75-year-old man had pancreatic cancer in the body of the pancreas. **a** Contrast-enhanced computed tomography shows the pancreatic cancer as a hypodense area (*white arrows*). Dilatation of the upper stream main pancreatic duct is also present. **b** On the axial fat-suppressed T2-weighted MR image, a pancreatic body mass (*white arrows*) is observed as a slightly hyperintense area surrounding a marked hyperintense area (*white arrowhead*). The *open arrow* indicates residual normal parenchyma. This lesion is categorized as the target type. **c** On the axial precontrast fat-suppressed T1-weighted MR image, a pancreatic body mass (*white arrows*) is observed as a homogeneously hypointense area. The *open arrow* indicates residual normal parenchyma. This lesion is categorized as the homogeneous type. **d** On the axial pancreatic phase dynamic contrast-enhanced fat-suppressed T1-weighted MR image, a pancreatic body mass is apparent as a hypointense area (*white arrows*) with a central poorly enhanced area (*white arrowhead*). The *open arrow* indicates residual normal parenchyma. This lesion is categorized as the target type. **e** On the axial equilibrium phase dynamic contrast-enhanced fat-suppressed T1-weighted MR image, a pancreatic body mass is apparent as a slightly hypointense area (*white arrows*) with a central poorly enhanced area (*white arrowhead*). The *open arrow* indicates residual normal parenchyma. This lesion is categorized as the target type

precontrast T1WI or pancreatic phase DCE-T1WI, supporting our reasoning. However, in most of the speckled type f-AIP lesions on precontrast T1WI, the speckled hyperintense areas were not consistent with the speckled enhancement on pancreatic phase DCE-T1WI. We suspect that mismatch between these two sequences may have been caused by inappropriate timing of normal pancreatic parenchymal enhancement on pancreatic phase DCE-T1WI, although optimum timing for pancreatic phase should have been established in our procedure.

The speckled type f-AIP on T2WI and on precontrast T1WI indicated high accuracy in our study (Table 2) and is also regarded a useful finding, although the sensitivity was low. We suspect that insufficient contrast between the pancreatic lesion and residual normal pancreatic lobules on T2WI and precontrast T1WI may have reduced the

Table 5 Distributions of MR findings previously reported for pancreatic lesions

MR findings	No. of lesions (%)	
	Autoimmune pancreatitis ($n = 20$)	Pancreatic cancer ($n = 40$)
Unclear margin	19 (95.0)	37 (92.5)
Vascular involvement	12 (60.0)	31 (73.8)
Capsule-like rim	2 (10.0)	0 (0)
Duct-penetrating sign[a]	2 (12.5)	3 (8.1)
Pancreatic duct dilatation[a]	3 (23.1)	26[†] (74.3)

[†] $P < 0.001$; the number of lesions is significantly larger than for the other disease

[a] MR cholangiopancreatography was performed for 15 focal autoimmune pancreatitis patients and 35 pancreatic cancer patients

sensitivity. In our study, 6/10 speckled type f-AIP on T2WI were of the same type on precontrast T1WI and we could find no lesion with speckled hyperintense areas on T2WI consistent with that on precontrast T1WI and pancreatic phase DCE-T1WI. Thus, the speckled hyperintense areas within f-AIP lesions on T2WI may not have reflected normal pancreatic lobules, unlike those on precontrast T1WI and pancreatic phase DCE-T1WI. We suspect that the speckled hyperintense areas within f-AIP lesions on T2WI may have reflected inhomogeneous inflammatory changes; pathologic confirmation will be required to prove this.

The homogeneous type PC lesions on T2WI and on precontrast T1WI were observed significantly more frequently in f-AIP in this study (Table 1). However, we regard these findings of little use in differentiating between f-AIP and PC because of their low specificity.

Compared with the enhancement of the normal pancreas, generally diminished vascularity and poor enhancement in the early phase and gradual enhancement in the late phase are observed for pancreatic adenocarcinoma. Mitchel et al. [38] and Gabata et al. [39] reported that focal pancreatic lesions such as PC had been clearly demonstrated as hypointense areas on precontrast T1WI or pancreatic phase DCE-T1WI. Other previous reports suggested that these MR features reflected fibrous stroma or marked desmoplastic reaction with formation of dense fibrous tissue as pathological findings of typical pancreatic ductal adenocarcinoma [40–43]. Wakabayashi et al. [34] reported that less tumor enhancement was frequently observed for PC, and this included a poorly attenuated area, reflecting necrosis and bleeding, on the delayed images. In our study, the target type MR features (hypointensity to hyperintensity surrounding a less enhanced focal area) on pancreatic phase and equilibrium phase DCE-T1WI were seen significantly more frequently in PC than in f-AIP (Table 1) and their specificity for diagnosis of PC was 100%; any f-AIP lesion did not show this type. This result suggests that we may be able to exclude f-AIP when a focal pancreatic lesion is seen as the target type (hypointensity to hyperintensity surrounding a less enhanced area) on contrast-enhanced MRI. We suspect that an internal less enhanced area of the target type PC on DCE-T1WI reflects a marked desmoplastic reaction and that a marginal zone of a lesion reflects a peritumoral area of inflammatory cell invasion or fibrous tissue. The effect of contrast enhancement of the marginal zone may have varied depending on the extent of those pathologic conditions. In our study, seven PC lesions had the target type MR feature on T2WI (hyperintensity surrounding a more hyperintense focal area) and the same type of MR feature (hypointensity to hyperintensity surrounding a less enhanced focal area) was observed for four of these on pancreatic phase and equilibrium phase DCE-T1WI. According to Wakabayashi et al. [34] and Hattori et al. [44], in such PC cases, an internal hyperintense area of the target type PC on T2WI, which was less enhanced on DCE-T1WI, may have reflected cystic, necrotic, and mucinous components or bleeding whereas these pathologic conditions are uncommon in AIP.

The homogeneous type of PC on T2WI and precontrast T1WI were also seen significantly more frequently than f-AIP in our study. However, these MR features were regarded as of little use in differentiating between f-AIP and PC because of their low specificity.

Okamoto et al. [45] reported that tiny spotty or irregular heterogeneous enhanced lesions within the PC at the perfusion image phase had correlated with small vessels at the vascular image phase on contrast-enhanced ultrasonography. In our study, four PC cases had the speckled type MR feature on pancreatic phase or equilibrium phase DCE-T1WI and the speckled enhanced areas within these lesions may have coincided with heterogeneous enhanced areas depicted in the above-mentioned report [45]. The speckled type MR feature on all of the sequences indicated high specificity for diagnosis of f-AIP in our study and it may be difficult to distinguish this type of PC from f-AIP. However, the speckled hyperintense areas seen in such PC lesions did not correspond to those on the other sequences. The case shown in Fig. 5 showed the speckled type MR feature on precontrast T1WI and the target type on DCE-T1WI. If the target type MR finding is observed on any other sequence, we may exclude f-AIP because the target type is regarded as specific to PC. Hence, we believe that we are able to distinguish such PC cases from f-AIP by careful review of all sequences. Additionally, when upper stream MPD dilatation, reported to be a sign of high risk of PC [35, 46–48], is observed, a focal pancreatic mass is

more likely to be cancer. In our study, dilatation of the upper stream MPD was observed significantly more frequently in PC than in f-AIP ($P < 0.001$) and this finding is believed to be suggestive of PC, and although pancreatic duct dilatation is observed even in elderly patients [49], age difference would have not affected the results of our study.

In this study there was a discrepancy between 2D-T1WI and 3D-T1WI in distribution with regard to several types of pancreatic lesion, for example the homogeneous type on precontrast T1WI and equilibrium phase DCE-T1WI, the speckled type on equilibrium phase DCE-T1WI, and the target type on precontrast T1WI (Table 3). We attributed this to the small number of respective cases on 2D-T1WI and on 3D-T1WI.

Our study had some limitations. The main was its retrospective nature. Prospective studies would be more definitive for identifying MR findings that can differentiate f-AIP from PC. Second, only two possible diagnoses were allowed in the cohort, the number of patients was limited, and there was a significant difference between the mean diameters of the lesions. Third, the effects of two different magnetic field strengths, 1.5 and 3.0 T, and of two different type T1-weighted sequences, 2D-T1WI and 3D-T1WI, might have been overlooked, because this study was not quantitative. Actually, the characteristic MR finding, speckled hyperintensity on pancreatic phase DCE-T1WI, enabled highly accurate diagnosis of f-AIP whether on 2D or 3D sequence (although the accuracy on 3D sequence was higher than that on 2D) (Table 4). Fourth, correlation between histopathological findings and MR features of the lesions was not attempted.

In summary, we identified a characteristic MR finding that can discriminate f-AIP from PC. It was speckled or dotted enhancement within a hypointense or isointense lesion on pancreatic phase DCE-T1WI. In addition, speckled or dotted hyperintensity within a hypointense or isointense lesion on T2WI and on precontrast T1WI was also a useful MR finding despite its low sensitivity. The MR features previously reported as characteristic of AIP, for example capsule-like rim and duct penetrating sign, may not be useful in differentiating f-AIP and PC because of low sensitivity, but may be specific. Serum IgG4 levels were elevated in most of our f-AIP patients and specificity for diagnosis of f-AIP was high. We may be able to avoid unnecessary EUS-FNA or surgery for a focal AIP mass suspected of being PC when the above MR findings are observed with elevated serum IgG4. On the other hand, hypointensity to hyperintensity surrounding a less enhanced focal area on DCE-T1WI that accompanies the dilatation of upper stream MPD on MRCP is suggestive of PC. Accordingly, we believe MR imaging to be a valuable diagnostic tool for differentiation of f-AIP from localized PC.

Acknowledgments We thank Takeshi Uehara, Department of Laboratory Medicine, Shinshu University School of Medicine for comments on the pathology. This work was supported by a Grant-in Aid for Scientific Research (C) (20590805) from the Japan Society for the Promotion of Science.

References

1. Toki F, Kozu T, Oi I, Nakasato T, Suzuki M, Hanyu F. An unusual type of chronic pancreatitis showing diffuse irregular narrowing of the entire main pancreatic duct on ERCP—a report of four cases. Endoscopy. 1992;24:640 (abstract).
2. Yoshida K, Toki F, Takeuchi T, Watanabe S, Shiratori K, Hayashi N. Chronic pancreatitis caused by an autoimmune abnormality. Proposal of the concept of autoimmune pancreatitis. Dig Dis Sci. 1995;40:1561–8.
3. Ito T, Nakano I, Koyanagi S, Miyahara T, Migita Y, Ogoshi K, et al. Autoimmune pancreatitis as a new clinical entity. Three cases of autoimmune pancreatitis with effective steroid therapy. Dig Dis Sci. 1997;42:1458–68.
4. Wakabayashi T, Motoo Y, Kojima Y, Makino H, Sawabu N. Chronic pancreatitis with diffuse irregular narrowing of the main pancreatic duct. Dig Dis Sci. 1998;43:2415–25.
5. Horiuchi A, Kawa S, Akamatsu T, Aoki Y, Mukawa K, Furuya N, et al. Characteristic pancreatic duct appearance in autoimmune chronic pancreatitis: a case report and review of the Japanese literature. Am J Gastroenterol. 1998;93:260–3.
6. Erkelens GW, Vleggaar FP, Lesterhuis W, van Buuren HR, van der Werf SD. Sclerosing pancreato-cholangitis responsive to steroid therapy. Lancet. 1999;354:43–4.
7. Hamano H, Kawa S, Horiuchi A, Unno H, Furuya N, Akamatsu T, et al. High serum IgG4 concentrations in patients with sclerosing pancreatitis. N Engl J Med. 2001;344:732–8.
8. Hamano H, Kawa S, Ochi Y, Unno H, Shiba N, Wajiki M, et al. Hydronephrosis associated with retroperitoneal fibrosis and sclerosing pancreatitis. Lancet. 2002;359:1403–4.
9. Okazaki K, Chiba T. Autoimmune related pancreatitis. Gut. 2002; 51:1–4.
10. Sahani DV, Kalva SP, Farrell J, Maher MM, Saini S, Mueller PR, et al. Autoimmune pancreatitis: imaging features. Radiology. 2004;233:345–52.
11. Yang DH, Kim KW, Kim TK, Park SH, Kim SH, Kim MH, et al. Autoimmune pancreatitis: radiologic findings in 20 patients. Abdom Imaging. 2006;31:94–102.
12. Chari ST, Smyrk TC, Levy MJ, Topazian MD, Takahashi N, Zhang L, et al. Diagnosis of autoimmune pancreatitis: the Mayo Clinic experience. Clin Gastroenterol Hepatol. 2006;4:1010–6 (quiz 934).
13. Irie H, Honda H, Baba S, Kuroiwa T, Yoshimitsu K, Tajima T, et al. Autoimmune pancreatitis: CT and MR characteristics. AJR Am J Roentgenol. 1998;170:1323–7.
14. Furukawa N, Muranaka T, Yasumori K, Matsubayashi R, Hayashida K, Arita Y. Autoimmune pancreatitis: radiologic findings in three histologically proven cases. J Comput Assist Tomogr. 1998;22:880–3.
15. Servais A, Pestieau SR, Detry O, Honore P, Belaiche J, Boniver J, et al. Autoimmune pancreatitis mimicking cancer of the head of pancreas: report of two cases. Acta Gastroenterol Belg. 2001;64: 227–30.
16. Hardacre JM, Iacobuzio-Donahue CA, Sohn TA, Abraham SC, Yeo CJ, Lillemoe KD, et al. Results of pancreaticoduodenectomy for lymphoplasmacytic sclerosing pancreatitis. Ann Surg. 2003; 237:853–8 (discussion 8–9).
17. Kamisawa T, Egawa N, Nakajima H, Tsuruta K, Okamoto A, Kamata N. Clinical difficulties in the differentiation of

autoimmune pancreatitis and pancreatic carcinoma. Am J Gastroenterol. 2003;98:2694–9.
18. Yadav D, Notahara K, Smyrk TC, Clain JE, Pearson RK, Farnell MB, et al. Idiopathic tumefactive chronic pancreatitis: clinical profile, histology, and natural history after resection. Clin Gastroenterol Hepatol. 2003;1:129–35.
19. Abraham SC, Wilentz RE, Yeo CJ, Sohn TA, Cameron JL, Boitnott JK, et al. Pancreaticoduodenectomy (Whipple resections) in patients without malignancy: are they all 'chronic pancreatitis'? Am J Surg Pathol. 2003;27:110–20.
20. Mizuno N, Bhatia V, Hosoda W, Sawaki A, Hoki K, Hara K, et al. Histological diagnosis of autoimmune pancreatitis using EUS-guided trucut biopsy: a comparison study with EUS-FNA. J Gastroenterol. 2009;44:742–50.
21. Horwhat JD, Paulson EK, McGrath K, Branch MS, Baillie J, Tyler D, et al. A randomized comparison of EUS-guided FNA versus CT or US-guided FNA for the evaluation of pancreatic mass lesions. Gastrointest Endosc. 2006;63:966–75.
22. Okazaki K, Kawa S, Kamisawa T, Naruse S, Tanaka S, Nishimori I, et al. Clinical diagnostic criteria of autoimmune pancreatitis: revised proposal. J Gastroenterol. 2006;41:626–31.
23. Hua YP, Liang LJ, Peng BG, Li SQ, Huang JF. Pancreatic head carcinoma: clinical analysis of 189 cases. Hepatobiliary Pancreat Dis Int. 2009;8:79–84.
24. Japan Pancreas Society. Classification of pancreatic carcinoma. 6th ed. Tokyo: Kanahara & Co.; 2009.
25. Ichikawa T, Sou H, Araki T, Arbab AS, Yoshikawa T, Ishigame K, et al. Duct-penetrating sign at MRCP: usefulness for differentiating inflammatory pancreatic mass from pancreatic carcinomas. Radiology. 2001;221:107–16.
26. Takahashi N, Fletcher JG, Fidler JL, Hough DM, Kawashima A, Chari ST. Dual-phase CT of autoimmune pancreatitis: a multireader study. AJR Am J Roentgenol. 2008;190:280–6.
27. Kawamoto S, Siegelman SS, Hruban RH, Fishman EK. Lymphoplasmacytic sclerosing pancreatitis (autoimmune pancreatitis): evaluation with multidetector CT. Radiographics. 2008;28:157–70.
28. Edge MD, Hoteit M, Patel AP, Wang X, Baumgarten DA, Cai Q. Clinical significance of main pancreatic duct dilation on computed tomography: single and double duct dilation. World J Gastroenterol. 2007;13:1701–5.
29. Ghazale A, Chari ST, Smyrk TC, Levy MJ, Topazian MD, Tkahashi N, et al. Value of serum IgG4 in the diagnosis of autoimmune pancreatitis and in distinguishing it from pancreatic cancer. Am J Gastroenterol. 2007;102:1646–53.
30. Raina A, Krasinskas AM, Greer JB, Lamb J, Fink E, Moser AJ, et al. Serum immunoglobulin G fraction 4 levels in pancreatic cancer: elevations not associated with autoimmune pancreatitis. Arch Pathol Lab Med. 2008;132:48–53.
31. Aalberse RC, Van Milligen F, Tan KY, Stapel SO. Allergen-specific IgG4 in atopic disease. Allergy. 1993;48:559–69.
32. Hussain R, Poindexter RW, Ottesen EA. Control of allergic reactivity in human filariasis. Predominant localization of blocking antibody to the IgG4 subclass. J Immunol. 1992;148:2731–7.
33. Shirakata Y, Shiraishi S, Sayama K, Miki Y. Subclass characteristics of IgG autoantibodies in bullous pemphigoid and pemphigus. J Dermatol. 1990;17:661–6.
34. Wakabayashi T, Kawaura Y, Satomura Y, Watanabe H, Motoo Y, Okai T, et al. Clinical and imaging features of autoimmune pancreatitis with focal pancreatic swelling or mass formation: comparison with so-called tumor-forming pancreatitis and pancreatic carcinoma. Am J Gastroenterol. 2003;98:2679–87.
35. Kim JK, Altun E, Elias J Jr, Pamuklar E, Rivero H, Semelka RC. Focal pancreatic mass: distinction of pancreatic cancer from chronic pancreatitis using gadolinium-enhanced 3D-gradient-echo MRI. J Magn Reson Imaging. 2007;26:313–22.
36. Fujinaga Y, Kadoya M, Hamano H, Kawa S, Momose M, Kawakami S, et al. Radiologic findings of IgG4-related disease. Curr Immunol Rev. 2011;7:186–203.
37. Chandan VS, Iacobuzio-Donahue C, Abraham SC. Patchy distribution of pathologic abnormalities in autoimmune pancreatitis: implications for preoperative diagnosis. Am J Surg Pathol. 2008;32:1762–9.
38. Mitchell DG, Vinitski S, Saponaro S, Tasciyan T, Burk DL Jr, Rifkin MD. Liver and pancreas: improved spin-echo T1 contrast by shorter echo time and fat suppression at 1.5 T. Radiology. 1991;178:67–71.
39. Gabata T, Matsui O, Kadoya M, Yoshikawa J, Miyayama S, Takashima T, et al. Small pancreatic adenocarcinomas: efficacy of MR imaging with fat suppression and gadolinium enhancement. Radiology. 1994;193:683–8.
40. Mergo PJ, Helmberger TK, Buetow PC, Helmberger RC, Ros PR. Pancreatic neoplasms: MR imaging and pathologic correlation. Radiographics. 1997;17:281–301.
41. Nishiharu T, Yamashita Y, Abe Y, Mitsuzaki K, Tsuchigame T, Nakayama Y, et al. Local extension of pancreatic carcinoma: assessment with thin-section helical CT versus with breath-hold fast MR imaging—ROC analysis. Radiology. 1999;212:445–52.
42. Obuz F, Dicle O, Coker A, Sagol O, Karademir S. Pancreatic adenocarcinoma: detection and staging with dynamic MR imaging. Eur J Radiol. 2001;38:146–50.
43. Vachiranubhap B, Kim YH, Balci NC, Semelka RC. Magnetic resonance imaging of adenocarcinoma of the pancreas. Top Magn Reson Imaging. 2009;20:3–9.
44. Hattori Y, Gabata T, Zen Y, Mochizuki K, Kitagawa H, Matsui O. Poorly enhanced areas of pancreatic adenocarcinomas on late-phase dynamic computed tomography: comparison with pathological findings. Pancreas. 2010;39:1263–70.
45. Okamoto Y, Kawamoto H, Takaki A, Ishida E, Ogawa T, Kuwaki K, et al. Contrast-enhanced ultrasonography depicts small tumor vessels for the evaluation of pancreatic tumors. Eur J Radiol. 2007;61:163–9.
46. Karasawa E, Goldberg HI, Moss AA, Federle MP, London SS. CT pancreatogram in carcinoma of the pancreas and chronic pancreatitis. Radiology. 1983;148:489–93.
47. Tanaka S, Nakaizumi A, Ioka T, Oshikawa O, Uehara H, Nakao M, et al. Main pancreatic duct dilatation: a sign of high risk for pancreatic cancer. Jpn J Clin Oncol. 2002;32:407–11.
48. Gangi S, Fletcher JG, Nathan MA, Christensen JA, Harmsen WS, Crownhart BS, et al. Time interval between abnormalities seen on CT and the clinical diagnosis of pancreatic cancer: retrospective review of CT scans obtained before diagnosis. Am J Roentgenol. 2004;182:897–903.
49. Glaser J, Stienecker K. Pancreas and aging: a study using ultrasonography. Gerontology. 2000;46:93–6.